Acoustic-mode vibrational anharmonicity related to the anomalous thermal expansion of Invar iron alloys

Ll. Mañosa,* G. A. Saunders, and H. Rahdi
School of Physics, University of Bath, Claverton Down, Bath BA2 7AY, United Kingdom

U. Kawald, J. Pelzl, and H. Bach
Institut für Experimentalphysik, Ruhr-Universität Bochum, Bochum, Germany
(Received 24 September 1991)

Measurements of the temperature dependences of the hydrostatic-pressure derivatives of the velocities of ultrasonic waves propagated in single crystals of the Invars $Fe_{72}Pt_{28}$ and $Fe_{72}Pt_{25}Ni_3$ verify that the negative thermal expansion in the ferromagnetic phase of these alloys is directly associated with longitudinal-acoustic-mode softening. In the paramagnetic phase of $Fe_{72}Pt_{28}$, the hydrostatic-pressure derivatives of each of the elastic-tensor components and the bulk modulus B are positive, showing normal behavior in the sense that the long-wavelength acoustic-phonon frequencies increase under pressure. However, below the Curie temperature T_C the velocities of longitudinal untrasonic waves propagated along the [100] and [110] directions in $Fe_{72}Pt_{28}$ and $Fe_{72}Pt_{25}Ni_3$ decrease strongly with pressure; thus $(\partial C_{11}/\partial P)_{P=0}$, $(\partial C_L/\partial P)_{P=0}$, and $(\partial B^S/\partial P)_{P=0}$ are negative due to the magnetoelastic interaction. These Invar alloys show the extraordinary property of becoming easier to compress as the pressure is increased. The negative signs of $(\partial C_{11}/\partial P)_{P=0}$ and $(\partial C_L/\partial P)_{P=0}$ give rise to negative values for all the longitudinal- and quasilongitudinal-acoustic-mode Grüneisen parameters in the ferromagnetic phase. This experimental observation is in accord with a recent prediction of negative longitudinal-acoustic-mode Grüneisen parameters stemming from itinerant-electron-magnetism theory. For $Fe_{72}Pt_{28}$ the hydrostatic-pressure derivative $(\partial C_{11}/\partial P)_{P=0}$ is negative, attains its maximum value just above room temperature, and becomes much smaller as the temperature is lowered, matching, and accounting for, the behavior of the thermal expansion, which is negative in the temperature range between about 260 K and the Curie temperature. In the case of the archetypal Invar alloy $Fe_{65}Ni_{35}$, the hydrostatic-pressure derivatives of the elastic-stiffness-tensor components are positive, but $(\partial C_{11}/\partial P)_{P=0}$ and $(\partial C_L/\partial P)_{P=0}$ are small in the ferromagnetic phase, consistent with its small but positive thermal expansion. It is concluded that longitudinal-acoustic-mode softening due to the magnetoelastic interaction is the source of the Invar behavior of each of these iron alloys. In addition, measurements of the temperature dependences of the ultrasonic wave velocities establish that the fcc-bct martensitic phase transition in Fe-Ni and Fe-Pt alloys is driven by a soft shear zone-center acoustic phonon with propagation vector $\langle 110 \rangle$ and polarization vector $\langle 1\bar{1}0 \rangle$.

I. INTRODUCTION

The Invar problem is of long standing. Guillaume[1] discovered the original "Invar" property that fcc Fe-Ni alloys containing about 35 at. % Ni have a nearly constant (invariant) thermal expansion in a wide region around room temperature; subsequently he found the temperature-independent elastic behavior of Fe-Ni-Cr alloys—the "Elinvar" effect.[2] He was awarded the Nobel Prize in 1920 "in recognition of the services he has rendered to precise measurements in Physics by his discovery of anomalies in nickel steel alloys." Despite intensive research efforts on Invar effects, their microscopic origin and relationship to magnetoelasticity has remained an issue of controversial debate.[3–8] Recently we have observed[9,10] a phenomenon pivotal to an understanding of the Invar question: the velocities of longitudinal ultrasonic modes decrease when hydrostatic pressure is applied to the ferromagnetic Invar alloy $Fe_{72}Pt_{28}$. Although $(\partial C_{11}/\partial P)_{P=0}$ and $(\partial C_L/\partial P)_{P=0}$ [where $C_L(=(C_{11}+C_{12}+2C_{44})/2)$] are positive in the paramagnetic phase, both are negative in the ferromagnetic phase of $Fe_{72}Pt_{28}$.[9,10] Below the Curie temperature T_C $(\partial C_{11}/\partial P)_{P=0}$ and $(\partial C_L/\partial P)_{P=0}$ are negative due to a magnetoelastic interaction. A second recently recognized property to be added to the diverse range of anomalous properties that constitute aspects of Invar behavior[3,5,11–13] is that for $Fe_{72}Pt_{28}$ the bulk modulus decreases with pressure: this material shows the extraordinary feature of becoming easier to squeeze when pressure is applied to it.[10] Thus ultrasonic studies under pressure have provided the first experimental evidence for negative longitudinal acoustic mode Grüneisen parameters in the ferromagnetic phase—as suggested[6] independently on the basis of itinerant electron magnetism theory—an observation that is directly pertinent to the Invar problem accounting[10] for the negative thermal expansion observed[14] in $Fe_{72}Pt_{28}$.

A thermodynamic property such as thermal expansion, which is a consequence of atomic thermal motion, must

be governed by the anharmonicity of lattice vibrations incorporating contributions from phonons of wave vectors **k** which span the entire Brillouin zone in each branch p of the dispersion curves. In the quasiharmonic approximation the thermal Grüneisen parameter γ^{th}, a widely used measure of net vibrational anharmonicity, is related to the volume thermal expansion α_V and specific heat C by

$$\gamma^{\text{th}}=\frac{\alpha_V V B^S}{C_P}=\frac{\alpha_V V B^T}{C_V}\ , \tag{1}$$

where B^S and B^T are the isentropic and isothermal bulk moduli, respectively. The thermal Grüneisen parameter γ^{th} is the weighted average of all the individual mode (i) Grüneisen parameters γ_i:

$$\gamma^{\text{th}}=\sum_i C_i\gamma_y \Big/ \sum_i C_i\ . \tag{2}$$

Measurements of the hydrostatic pressure derivatives of the elastic stiffness tensor components can be used to determine the Grüneisen parameters of the acoustic modes in the long-wavelength limit and so enable the effects of these modes to be separated from those of optical modes and higher-wave-vector acoustic modes. The discovery[9,10] of negative values for the longitudinal acoustic mode Grüneisen parameters indicates that the anomalous vibrational anharmonicity of these modes must be largely responsible for negative thermal expansion[14] of $Fe_{72}Pt_{28}$ between about 260 K and the Curie temperature T_C.

Magnetically induced volume changes are usually small in metals and alloys. Invar-type materials comprise the exception in that magnetic ordering produces very large volume effects, and in the Fe-Pt alloys below T_C these more than compensate the normal lattice expansion with the result that the net effect of vibrational anharmonicity is a negative thermal expansivity. In the Fe-Ni alloys compensation leads to a small thermal expansion, that of Fe–35 at. % Ni being close to zero around room temperature.[1] An important question is whether the concept of longitudinal acoustic mode softening induced by the magnetoelastic interaction can provide a single framework in which to accommodate the Invar behavior of the Fe-Ni as well as the Fe-Pt alloys. To examine this the program has included measurements of the $(\partial C_{IJ}/\partial P)_{P=0}$ for the classic Invar composition Fe–35 at. % Ni with instructive results. The work on Fe–35 at. % Ni complements that of Renaud[15] who measured the effects of hydrostatic pressure on the elastic constants for a range of Fe-Ni Invar alloys. However, the Invar anomaly is much more pronounced in Fe_3Pt, which has the largest negative thermal expansion in the Fe-Pt alloy system and so the central purpose here is to describe and discuss in detail the experimental results obtained for the pressure dependence of the velocities of ultrasonic modes propagated through $Fe_{72}Pt_{28}$. To examine a general proposition that longitudinal mode softening due to the magnetoelastic interaction is the source of the Invar behavior in iron alloys, the experimental study of the elastic behavior under pressure has been extended to $Fe_{72}Pt_{25}Ni_3$ another alloy which shows negative thermal expansion.[16]

Both the Fe-Ni and Fe-Pt Invar alloys show a lattice instability against a displacive transformation from a fcc to a bct martensite structure.[17] Ultrasonic wave velocity measurements provide a direct test of whether a displacive phase transition is accompanied by softening of a long-wavelength acoustic-phonon mode and so can be categorized as an elastic phase transition. Inspection of the data of Hausch and Warlimont[18] for the behavior of the elastic stiffnesses of Fe-Ni alloys with temperature reveals that the shear stiffness $(C_{11}-C_{12})/2$ is small and decreases even further as the Martensitic start temperature M_s is approached. For the Fe-Pt alloys $(C_{11}-C_{12})/2$ is also small.[4] In the case of $Fe_{25}Pt_{75}$ $(C_{11}-C_{12})/2$ becomes almost zero at 205 K where the ultrasonic echoes disappear abruptly so that this temperature can be identified as M_s.[19] These elastic stiffness tensor component measurements indicate that the symmetry breaking at the fcc-bct transition in Fe-Ni and Fe-Pt alloys is shear on $\langle 110\rangle$ planes in $\langle 1\bar{1}0\rangle$ directions driven by softening of the corresponding zone-center acoustic phonon.[10] This suggestion is now explored in detail by considering the effect of temperature on the elastic stiffness tensor components.

II. EXPERIMENTAL DETERMINATION OF THE TEMPERATURE DEPENDENCES OF THE HYDROSTATIC PRESSURE DERIVATIVES OF THE ELASTIC STIFFNESS TENSOR COMPONENTS

Large single crystals are required for precision measurements of ultrasonic wave velocities and their pressure dependences. Crystals of centimeter dimensions were grown by the Bridgman-Stockbarger process. The disordered $Fe_{72}Pt_{28}$ crystal becomes ferromagnetic at T_C of 367 K.[10] The $Fe_{72}Pt_{25}Ni_3$ alloy has a Curie temperature of 405 K.[19] Inspection of the phase diagram[20] for disordered Fe-Pt alloys shows that the fcc-bct martensitic phase transformation occurs for a composition just below 28 at. % Pt. However, a 28-at. % Pt alloy should remain fcc down to 4.2 K; the particular crystal of $Fe_{72}Pt_{28}$ whose results are discussed here does so.[19] Crystals were orientated on a three-arc goniometer to $\pm 0.5°$ using Laue back-reflection photography. Ultrasonic samples were cut and polished with two faces, normal to the required propagation direction, flat to surface irregularities of about 2 μm and parallel to better than 10^{-3} rad. Ultrasonic wave velocities measurements were made along [100] and [001] directions. X- and Y-cut quartz transducers were used to generate and detect 10-MHz ultrasonic pulses. Satisfactory acoustic coupling could be achieved above room temperature using Dow Resin 276-V9 and below room temperature with Nonaq stopcock grease. Ultrasonic pulse transit times were measured using the pulse-echo overlap technique[21] capable of resolution of velocity changes to 1 part in 10^6 and particularly well suited to the determination of pressure- or temperature-induced changes in velocity. Results were corrected for transducer diffraction effects using the methods developed by Kittinger.[22] Hydrostatic pressure was ap-

plied in a piston and cylinder apparatus sealed with Viton O rings. Silicone fluid was used as the pressure transmitting medium: the lowest temperature at which experiments could be made was limited by the stringent requirement that the pressure transmitting oil must remain liquid to ensure hydrostatic conditions. Temperatures above room temperature were reached within the pressure cell by using a heating element wrapped around the outside of the pressure cylinder. During pressure runs it was essential to ensure that velocity measurements were made at the same controlled temperature ($\pm 0.1\,^{\circ}C$) because ultrasonic wave velocity depends strongly upon temperature. The pressure was measured using the change in resistance of a precalibrated manganin wire coil inside the cell. For further details of the experimental setup see Flower and Saunders.[23]

III. THE ELASTIC STIFFNESS TENSOR COMPONENTS AND THEIR TEMPERATURE DEPENDENCES

A quantitative description of the response of a material to stress requires knowledge of the second-order elastic constants (SOEC) and their behavior under pressure and temperature. Since anomalous elastic properties are an integral part of Invar behavior, they have been extensively studied before for Fe-Ni,[24,25,18,19] Fe-Pt,[4,19] and Fe-Pt-Ni[19] alloys. To obtain the temperature dependence of the pressure derivatives accurately, it is essential to measure the ultrasonic wave velocity and its temperature dependence as well as the change under pressure in the same crystals, especially for these alloys having composition sensitive elastic properties. This has been done here.

The adiabatic SOEC elastic stiffnesses for $Fe_{72}Pt_{28}$, $Fe_{72}Pt_{25}Ni_3$, and $Fe_{65}Ni_{35}$ are compared in Table I with data for related alloys obtained by other workers and those of the component elements Fe, Ni, and Pt. Before attempting to consider the ways in which the second-order elastic stiffness tensor components indicate special effects in the alloys, it may be well to recall the characteristics of simple solids. If the ions are sited at the centers of symmetry, as in a fcc crystal, and the interatomic potential is purely radial and independent of angle, then the Cauchy relationship $C_{12}=C_{44}$ should hold. Of course all metals, even the simplest but especially the transition elements, breach this, partly owing to the effect of volume dependent forces in severing the Cauchy relations, and partly owing to having noncentral forces. Usually fcc crystals exhibit marked shear anisotropy with $(C_{11}-C_{12})/2$ being substantially less than C_{44}. One intriguing feature of the Fe-Pt and Fe-Ni alloys is that C_{11} is much smaller than that in the elements. This diminished C_{11} [and $C_L(=(C_{11}+C_{12}+2C_{44})/2)$] as compared with the elements establishes that the long-wavelength longitudinal phonons are exceptionally soft. This is also a property of the antiferromagnetic $Mn_{85}Ni_9C_6$ and $Mn_{83}Ni_{11}C_6$ Invar alloys to the extent that C_{11} can be less than C_{44} so that the longitudinal ultrasound velocity is slower than that of the shear mode along a ⟨100⟩ direction.[28,29] If the martensite transition at low temperatures is destined to be cubic to tetragonal, noting the low value

TABLE I. Comparison between the room temperature (293 K) elastic properties of Fe-Ni-Pt alloys and those of the elements.

	Ni (Ref. 26)	Fe (Ref. 26)	Pt (Ref. 27)	$Fe_{64.7}Ni_{35.3}$ (Ref. 18)	$Fe_{65}Ni_{35}$	$Fe_{64}Ni_{36}$ (Ref. 15)	$Fe_{58}Ni_{42}$ (Ref. 15)	$Fe_{72}Pt_{28}$ (Ref. 4)	$Fe_{72}Pt_{28}$	$Fe_{72}Ni_3Pt_{25}$
Elastic stiffness constants (10 GPa)										
C_{11}^S	24.7	23.0	34.7	17.03	13.6	16.8	16.4	12.2	14.4	13.4
C_{44}	12.2	11.7	7.65	10.42	9.8	10.4	10.2	8.6	8.0	9.0
C_{12}^S	15.3	13.5	25.1	11.63	9.2	11.4	11.2	8.8	10.7	9.5
$\frac{1}{2}(C_{11}^S-C_{12}^S)$	4.7	4.7	4.8	2.7	2.2	2.7	2.6	1.7	1.8	1.9
Elastic compliances (10^{-2} GPa^{-1})										
S_{11}	0.769	0.767	0.735	1.32	7.73	1.31	1.37	2.07	1.9	1.8
S_{44}	0.820	0.857	1.31	0.96	1.02	0.96	0.98	1.16	1.25	1.1
S_{12}	−0.29	−0.28	−0.38	−0.53	-0.051	−0.53	−0.56	−0.86	−0.81	−0.7
Density (kg m^{-3})	8900	7873	21450	~8800	8121			11980	11939	11570
Bulk modulus B_0^S (10 GPa)	18.4	16.7	28.3	13.4	10.7	13.2	12.9	10.2	12.0	10.8
$(\partial C_{11}^S/\partial P)_{P=0}$	6.0	6.7	—	—	5.2	3.9	0.67	—	−19.2	−20.9
$(\partial C_{44}^S/\partial P)_{P=0}$	2.4	2.6	—	—	5.7	5.45	3.2	—	0.6	3.6
$(\partial C_{12}^S/\partial P)_{P=0}$	4.7	4.6	—	—	−2.1	−2.5	−1.9	—	−26.0	−31.9
$(\partial B_0^S/\partial P)_{P=0}$	5.3	5.3	—	—	0.3	−0.35	−1.05	—	−23.7	−28.2

of C_{11} one might ask why does it not take place by the obvious mechanism, namely, by softening of the $\langle 100 \rangle$ longitudinal vibrations? The answer stems from the fact that one consequence of a small value of C_{11} is that the shear stiffness $C'(=(C_{11}-C_{12})/2)$ is also reduced.

The elastic stiffness tensor components of each of the alloys $Fe_{72}Pt_{28}$ (Fig. 1), $Fe_{72}Pt_{25}Ni_3$ (Fig. 2), and $Fe_{65}Ni_{35}$ (Fig. 3) show the markedly anomalous elastic behavior with temperatures characteristic of these Invar iron alloys.[4,9,10,18,19,24] In particular the shear modulus $(C_{11}-C_{12})/2$ of each alloy decreases substantially with reducing temperature. In the cases of $Fe_{72}Pt_{28}$ (Table II) and $Fe_{72}Pt_{25}Ni_3$ (Table III) C_{44} also shows this anomalous reduction. For these alloys $(C_{11}-C_{12})/2$ is substantially smaller than C_{44}: the shear anisotropy ratio $[A=2C_{44}/(C_{11}-C_{12})]$ is large (Fig. 4). These alloys show little resistance to shear on a $\langle 110 \rangle$ plane in a $\langle 1\bar{1}0 \rangle$ direction. The temperature dependences of the shear anisotropy ratio C_{44}/C' (Fig. 4) show that for $Fe_{72}Pt_{28}$ and $Fe_{72}Pt_{25}Ni_3$ $(C_{11}-C_{12})/2$ decreases much faster than C_{44} but not for $Fe_{65}Ni_{35}$. Furthermore C_{44}/C' becomes very large for $Fe_{72}Pt_{25}Ni_3$ at low temperatures as $(C_{11}-C_{12})/2$ reduces as the martensitic start temperature M_s at 170 K for this alloy is approached. Previous measurements[19] of the ultrasonic wave velocities were made in $Fe_{72}Pt_{25}Ni_3$ down to 170 K by which temperature $(C_{11}-C_{12})/2$ in particular had become very small (about 2 GPa). Hence as the temperature is reduced the shear modes, especially that associated with C', soften. Decrease of C' to a small value evidences incipient shear instability against the fcc-fct transformation. The strong response to a shear in a $\langle 1\bar{1}0 \rangle$ direction on a $\langle 110 \rangle$ plane reveals that the low temperature fcc-fct transition has a ferroelastic mechanism at the atomic level with the soft mode being a $\langle 1\bar{1}0 \rangle$ polarized long-wavelength shear-acoustic phonon propagated in a $\langle 110 \rangle$ direction and the order parameter being the associated strain tensor $(2\eta_{33}-\eta_{33}-\eta_{11})/\sqrt{3}$ (in Lagrangian strain tensor components η_{ij}) spanning a one-dimensional nonidentical irreducible subspace.[30-33] The

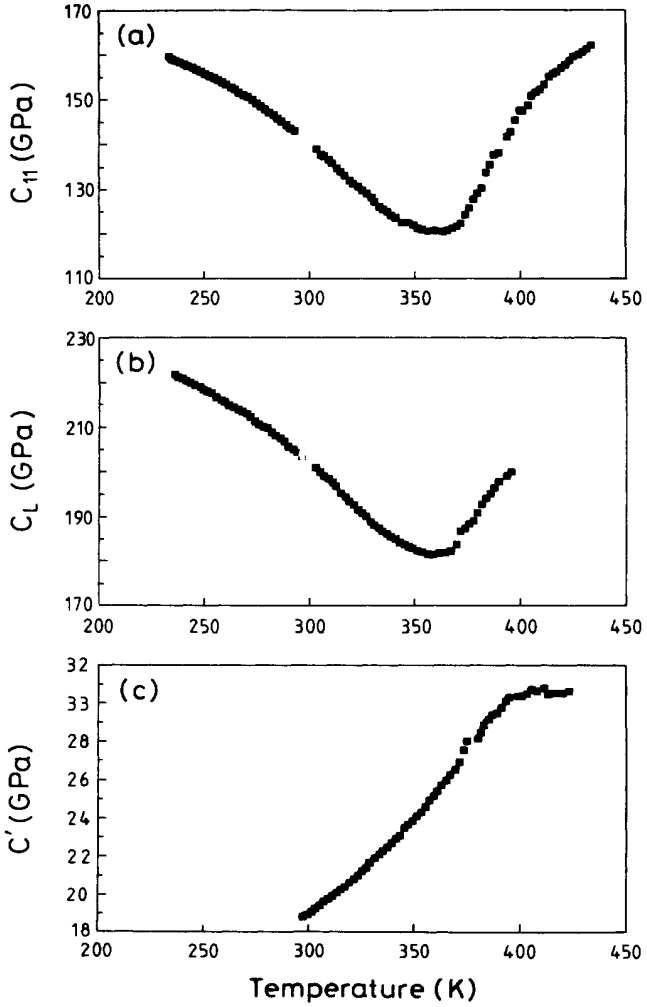

FIG. 1. The temperature dependences of the elastic stiffnesses (a) C_{11}, (b) $C_L(=(C_{11}+C_{12}+2C_{44})/2)$, and (c) $C'(=(C_{11}-C_{12})/2)$ of monocrystalline $Fe_{72}Pt_{28}$.

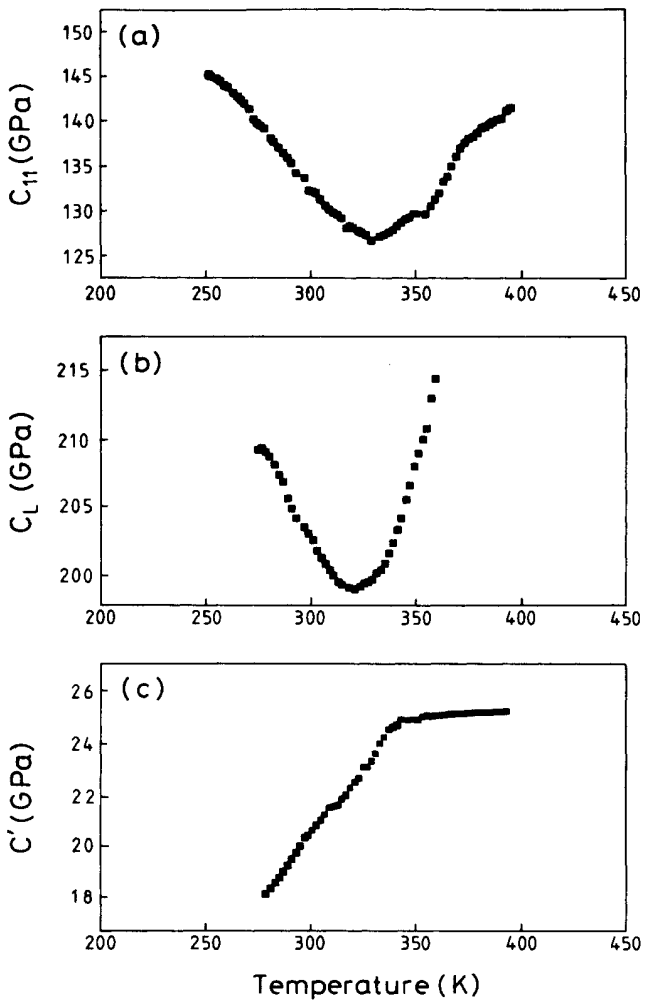

FIG. 2. The temperature dependences of the elastic stiffnesses (a) C_{11}, (b) C_L, and (c) C' of monocrystalline $Fe_{72}Pt_{25}Ni_3$.

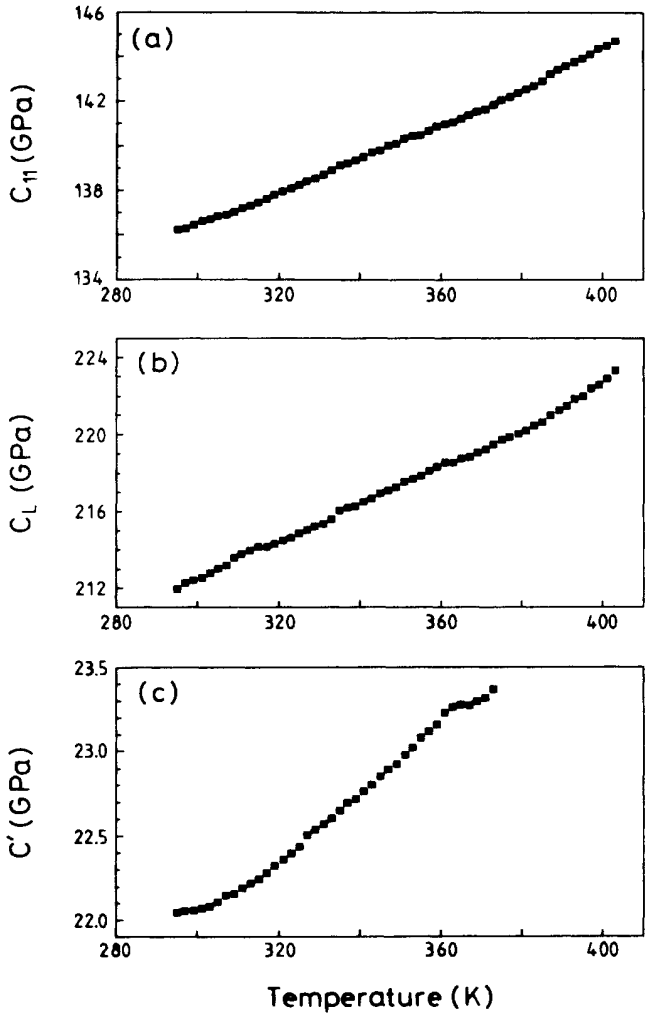

FIG. 3. The temperature dependences of the elastic stiffnesses (a) C_{11}, (b) C_L, and (c) C' of monocrystalline $Fe_{65}Ni_{35}$.

invariants of physical significance, which appear as powers and products of the basis vectors, are now required. The elastic free energy per unit mass expressed as a series in the finite Lagrangian strain tensor components η_{ij} for the cubic $m3m$ Laue group is

$$\Psi=\tfrac{1}{2}C_{11}(\eta_{11}^2+\eta_{22}^2+\eta_{33}^2)+C_{12}(\eta_{11}\eta_{22}+\eta_{11}\eta_{33}+\eta_{22}\eta_{33}) +\tfrac{1}{2}C_{44}(\eta_{12}^2+\eta_{13}^2+\eta_{23}^2)\ . \quad (3)$$

For a purely elastic transition it is necessary to work with symmetry-adapted strain tensor combinations, i.e., those which form bases for the irreducible representations. Hence expression (1) has been transformed under the invariance principle from the finite strain tensor space to an irreducible strain space spanned by six strain tensor components acting as eigenvectors:[30,31,34]

$$\begin{aligned}
&\eta_0^0=\eta_{11}+\eta_{22}+\eta_{33}\ ,\\
&\eta_1=(2\eta_{33}-\eta_{22}-\eta_{11})/\sqrt{3},\quad A\ ;\\
&\eta_1'=(2\eta_{11}-\eta_{33}-\eta_{22})/\sqrt{3}\ ;\\
&\eta_1''=(2\eta_{22}-\eta_{11}-\eta_{33})/\sqrt{3},\quad E\ ;\\
&\eta_2=\eta_{11}-\eta_{22},\quad \eta_2'=\eta_{22}-\eta_{33}\ ,\\
&\eta_{22}''=\eta_{33}-\eta_{11},\quad T\ ;\\
&\eta_3=\eta_{23},\quad \eta_4=\eta_{13},\quad \eta_5=\eta_{12}\ .
\end{aligned} \quad (4)$$

The strains η_0^0, (η_1,η_2), and (η_3,η_4,η_5) span three irreducible subspaces. η_0^0 represents a volume change, is invariant under the group symmetry elements, and spans a one-dimensional irreducible subspace. At lowest order η_1 is equal to $(c/\alpha-1)$; it describes a volume-conserving tetragonal $\langle 001\rangle$ distortion while η_2 is a shear in a $\langle 1\bar{1}0\rangle$ direction on a $\{110\}$ plane. In the irreducible strain-tensor space the Landau free energy to second order in Lagrangian strain is

$$\Psi=\tfrac{1}{6}(C_{11}+2C_{12})(\eta_0^0)^2+\tfrac{1}{4}(C_{11}-C_{12})(\eta_1^2+\eta_2^2) +\tfrac{1}{2}C_{44}(\eta_3^2+\eta_4^2+\eta_5^2)\ . \quad (5)$$

The observation that the shear stiffness $(C_{11}-C_{12})/2$ goes toward zero as M_s is approached indicates that the fcc-bct transition in these alloys is ferroelastic in nature and thus complies with the unified view that structural changes driven by zone center modes results from freezing in of the displacement of the atoms induced by the soft shear mode. The transition is ferrodistortive retaining the same number of atoms, one in this case, per unit cell.

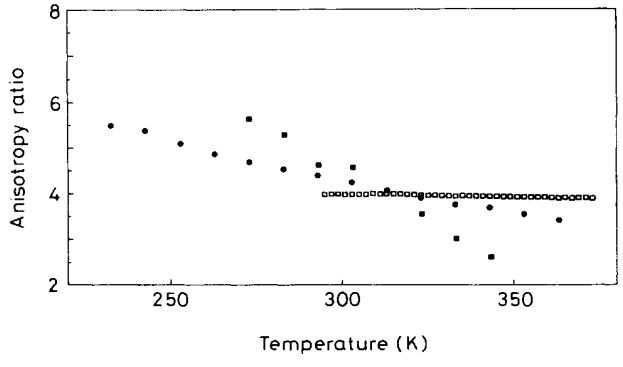

FIG. 4. The shear anisotropy ratio $A(=2C_{44}/(C_{11}-C_{12}))$ of $Fe_{72}Pt_{28}$ (solid circles), $Fe_{72}Pt_{25}Ni_3$ (solid squares), and $Fe_{65}Ni_{35}$ (open squares) as a function of temperature.

The temperature dependences of the velocities of longitudinal ultrasonic modes propagated along the [001] and [110] directions for $Fe_{72}Pt_{28}$ (Fig. 1) and $Fe_{72}Pt_{25}Ni_3$ (Fig. 2) are in accord with previous observations made by Hausch[4] on $Fe_{72}Pt_{28}$ that C_L $(=(C_{11}+C_{12}+2C_{44})/2)$ decreases to a minimum somewhat below the Curie temperature. For $Fe_{72}Pt_{28}$ and $Fe_{72}Pt_{25}Ni_3$ both C_{11} and C_L show magnetically induced decreases starting well above the Curie temperature. The position of the similar minimum observed for Fe-Ni alloys does not shift appreciably in a saturating magnetic field indicating that the source of the small values of C_{11} and C_L in the ferromagnetic state is an intrinsic magnetoelastic interaction rather than a domain-wall stress effect.[18] This is confirmed by observations of the minimum in the bulk modulus, determined from lattice parameter measurements—which should not be much affected by domain-wall

TABLE II. The second-order elastic stiffness tensor components, their hydrostatic pressure derivatives (obtained from the best fit to the experimental data), third-order elastic stiffness tensor component combinations, and mean elastic Grüneisen parameter of $Fe_{72}Pt_{28}$ at selected temperatures.

	Elastic stiffness (GPa)						Hydrostatic pressure derivatives						TOEC combinations ($\times 10^3$ GPa)			
T (K)	C_{11}	C_L	C'	C_{12}	C_{44}	B	$\frac{\partial C_{11}}{\partial P}$	$\frac{\partial C_L}{\partial P}$	$\frac{\partial C'}{\partial P}$	$\frac{\partial C_{12}}{\partial P}$	$\frac{\partial C_{44}}{\partial P}$	$\frac{\partial B}{\partial P}$	$C_{111}+2C_{112}$	$C_{144}+2C_{166}$	$C_{123}+2C_{112}$	γ^{el}
230	160.2	221.3	13.64	133	75	142	−6.0	−6.7	3.0	−12.0	2.3	−10.0	1.660	−1.386	4.846	1.6
240	158.2	219.8	14.35	130	76	139	−6.2	−6.7	3.0	−12.2	2.5	−10.2	1.750	−1.476	4.936	1.7
250	156.1	217.7	15.08	126	77	136	−8.0	−6.7	3.1	−14.2	4.4	−12.1	2.381	−2.107	5.567	2.5
260	153.6	214.8	15.83	122	77	132	−10.7	−8.5	3.1	−16.9	5.3	−14.8	3.373	−2.468	6.559	2.7
270	150.7	212.2	16.63	117	78	126	−14.0	−12.7	3.2	−20.4	4.5	−18.3	4.545	−2.107	7.732	1.9
280	147.4	208.9	17.42	113	79	124	−17.0	−17.2	3.3	−23.6	3.1	−21.4	5.627	−1.566	8.814	0.8
290	143.9	205.5	18.22	107	80	120	−19.2	−22.0	3.4	−26.0	0.6	−23.7	6.439	-0.664	9.625	−0.6
300	139.3	201.3	19.08	101	81	114	−21.5	−26.5	3.4	−28.2	−1.6	−26.0	7.251	0.147	10.44	−1.9
310	136.8	197.2	19.88	97	80	110	−23.0	−29.7	3.5	−30	−3.2	−27.7	7.792	0.799	10.98	−2.9
320	131.5	192.1	20.78	90	81	104	−23.2	−30.0	3.5	−30.2	−3.3	−27.9	7.882	0.779	11.07	−2.9
330	127.6	187.8	21.86	84	82	99	−21.7	−22.5	3.6	-28.9	2.8	−26.5	7.341	−1.386	10.53	0.1
340	123.7	184.8	22.84	78	84	97	−17.0	−13.7	3.7	−24.4	7.0	−21.9	5.627	−2.828	8.814	2.6
350	121.6	182.4	24.01	74	85	97	−10.5	−5.0	3.7	−17.9	9.2	−15.4	3.283	−3.640	6.464	4.4
360	120.7	181.8	25.34	70	86	87	−0.5	5.0	3.7	−7.9	9.2	−5.4	−0.324	−3.640	2.862	5.6

TABLE III. The second-order elastic stiffness tensor components, their hydrostatic pressure derivatives (obtained from the best fit to the experimental data), third-order elastic constants combinations, and mean elastic Grüneisen parameter γ^{el} for monocrystalline $Fe_{72}Pt_{25}Ni_3$ at selected temperatures.

	SOEC (GPa)						Pressure derivatives of SOEC						TOEC combinations (10^3 GPa)			
T (K)	C_{11}	C_L	C'	C_{12}	C_{44}	B	$\frac{\partial C_{11}}{\partial P}$	$\frac{\partial C_L}{\partial P}$	$\frac{\partial C'}{\partial P}$	$\frac{\partial C_{12}}{\partial P}$	$\frac{\partial C_{44}}{\partial P}$	$\frac{\partial B}{\partial p}$	$C_{111}+2C_{112}$	$C_{114}+2C_{166}$	$C_{123}+2C_{112}$	γ^{el}
290	134.4	204.5	19.5	95.4	89.6	108	−22.2	−19.7	6.2	−34.6	8.7	−30.4	6.76	−3.24	11.48	2.99
300	130.8	202.3	20.4	90.0	91.9	104	−19.2	−18.0	6.7	−32.6	7.9	−28.1	5.53	−2.86	10.35	2.81
310	128.5	200.5	21.8	84.9	93.8	99.4	−15.7	−14.0	7.0	−29.7	8.7	−25.0	4.26	−2.99	9.07	3.19
320	126.5	199.0	22.1	82.3	94.6	97.0	−10.5	−8.0	7.5	−25.5	10.0	−20.5	2.64	−3.30	7.63	4.07
330	125.4	199.8	23.1	79.0	97.6	94.5	−3.2	0.0	7.7	−18.6	10.9	−13.5	0.50	−3.47	5.48	4.75
340	125.0	202.1	24.2	76.6	101	92.7	8.5	15.0	8.0	−7.5	14.5	−2.2	−2.77	−4.41	2.29	6.62

effects.[35] The magnetic contribution increases with decreasing temperature below the Curie temperature until it more than counterbalances the usual anharmonic contribution at lower temperatures causing C_{11} and C_L to increase as the temperature is reduced. The minimum in C_{11} is located at lower temperatures for $Fe_{72}Pt_{25}Ni_3$ than for $Fe_{72}Pt_{28}$, implying that the magnetoelastic interaction for the former is weaker than for $Fe_{72}Pt_{28}$.

IV. THE HYDROSTATIC PRESSURE DERIVATIVES OF THE ELASTIC STIFFNESS TENSOR COMPONENTS AND THEIR TEMPERATURE DEPENDENCES

To study the effects of pressure on the elastic behavior of the alloys, the pressure dependence f' $(=df/dP)$ of the pulse echo overlap frequency f was measured for each ultrasonic mode at fixed temperature. In general the overlap frequency f was found to be linearly dependent upon pressure. The pressure derivative of the mode velocity was determined from[36]

$$(\rho V^2)' = \rho V_0^2 \left[\frac{2f'}{f} + \frac{1}{B_0} - 2S \right], \tag{6}$$

where ρ_0, B_0, and V_0 are the density, bulk modulus, and ultrasonic mode velocity, respectively, at atmospheric pressure. The effect of hydrostatic pressure on the natural velocity of ultrasonic waves was then determined. From the slopes of the pressure dependences of the natural velocity W, the hydrostatic pressure derivatives of the elastic constants have been calculated at atmospheric

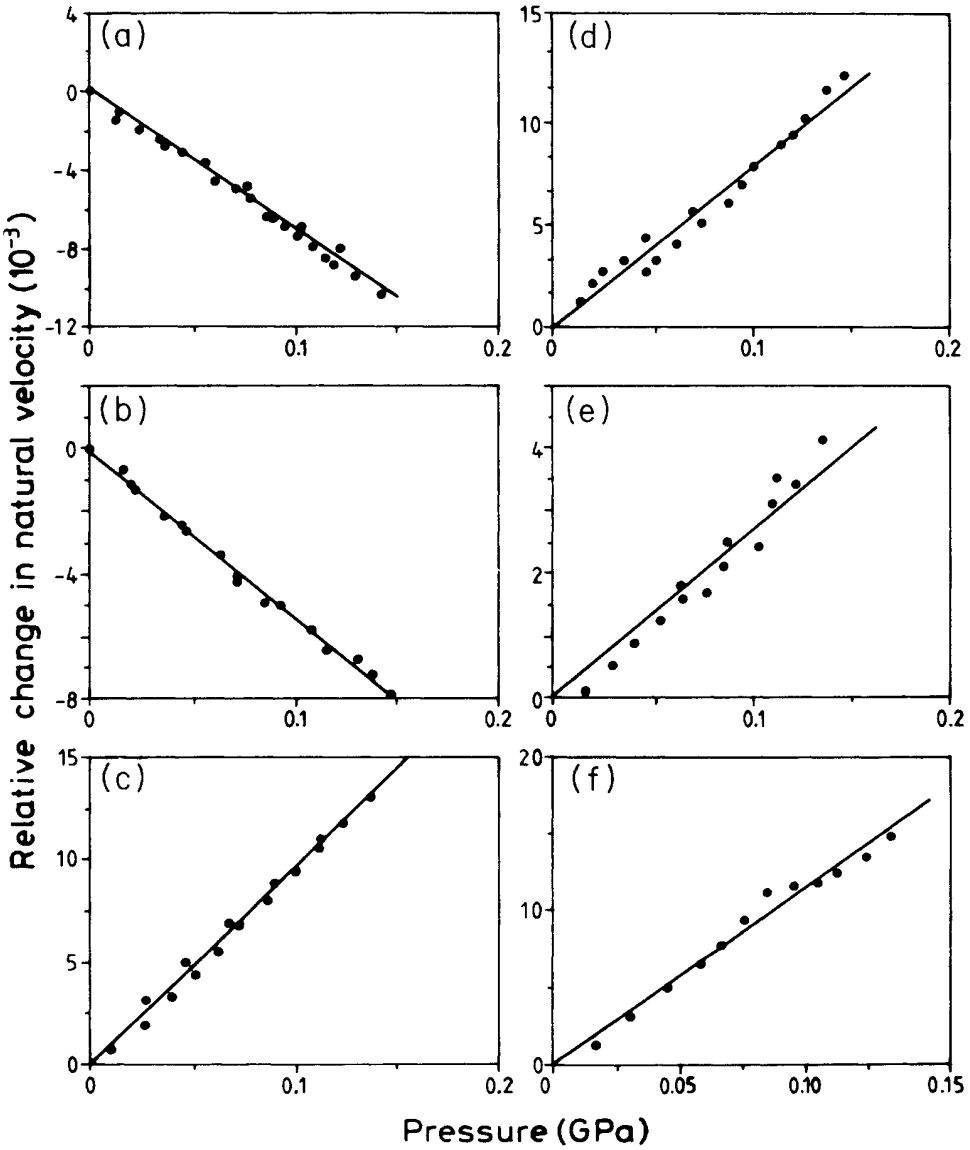

FIG. 5. The relative change with hydrostatic pressure in natural velocity of ultrasonic waves propagated in monocrystalline $Fe_{72}Pt_{28}$ in the ferromagnetic state at 293 K (a) **N**[001], **U**[001], (b) **N**[110], **U**[110], (c) **N**[110], **U**[1$\bar{1}$0], and in the vicinity of T_C at 360 K (d) **N**[001], **U**[001], (e) **N**[110], **U**[110], (f) **N**[110], **U**[1$\bar{1}$0]. Here **N** and **U** are the mode propagation and polarization vectors, respectively.

pressure by using

$$\left[\frac{\partial C_{IJ}}{\partial P}\right]_{T,P=0} = \frac{C_{IJ}}{(C_{11}^T + 2C_{12}^T)} + \frac{d(\rho_0 W^2)_{P=0}}{dP} . \quad (7)$$

A strikingly anomalous feature of the results obtained for $Fe_{72}Pt_{28}$ (Fig. 5) is that in the ferromagnetic state (typified here by the data obtained at 293 K) the velocities of the longitudinal modes propagated along the [001] and [110] directions decrease with increasing pressure [Figs. 5(a) and 5(b)]. The velocity of the $[1\bar{1}0]$ shear wave propagated down the [110] direction increases in the normal way under pressure. In the paramagnetic state each of the mode velocities shows the usual increase under pressure: the anomalous longitudinal mode softening is restricted to the ferromagnetic state. From the results obtained at 353 K just below the Curie temperature shown in Fig. 6 it can be seen that when pressure is applied so as to drive the crystal toward T_C (dT_c/dP is negative) the sign of the pressure dependence changes from negative to positive. The property that $(\partial C_{11}^S/\partial P)_{T,P}$ is equal to zero at a pressure of 0.7×10^8 Pa and 353 K is directly related to the minimum observed at 360 K in the temperature dependence of C_{11} (Fig. 1): this elastic stiffness has an extremum in T,P coordinate space. The anomalous negative pressure dependences of the velocities of longitudinal modes propagated along the [001] and [110] directions are also shown by $Fe_{72}Pt_{25}Ni_3$ in its ferromagnetic state [Figs. 7(a) and 7(b)], the velocity of the $[1\bar{1}0]$ shear wave propagated down the [110] direction again having the normal positive pressure gradient [Fig. 7(c)]. In the case of ferromagnetic $Fe_{65}Ni_{35}$ the velocities of longitudinal and shear modes each increase with pressure [Figs. 7(d)–7(f)]; this particular observation is not new: it was found by Renaud[15] who made measurements of the hydrostatic pressure derivatives of the elastic constants for Fe-Ni Invar alloys in the composition range 31.5 to 50 at. % Ni as a function of temperature from 77 to about 560 K. His results show that the $(\partial C_{IJ}/\partial P)_{P=0}$ and particularly $(\partial C_L/\partial P)_{P=0}$ vary enormously with temperature. In support of the suggestion[6,9,10] that the longitudinal acoustic mode softening plays the crucial role in causing Invar behavior is the observation in the present work that the alloy containing 35 at. % Ni, which has the smallest thermal expansion has a comparatively small value (6.17 at room temperature) of $(\partial C_L/\partial P)_{P=0}$. Furthermore Renaud[15] found an even smaller $(\partial C_L/\partial P)_{P=0}$ value (2.58) for the 42 at. % Ni alloy.

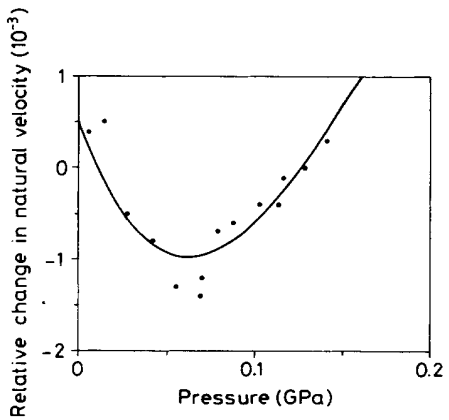

FIG. 6 The relative change induced by hydrostatic pressure in natural velocity of the longitudinal ultrasonic waves propagated along the [001] direction in monocrystalline $Fe_{72}Pt_{28}$ at 353 K, which is just below T_C. The application of pressure drives the crystal toward the Curie point.

The hydrostatic pressure derivatives $(\partial C_{IJ}^S/\partial P)_{P=0}$ of the elastic stiffness tensor components of $Fe_{72}Pt_{28}$, $Fe_{72}Pt_{25}Ni_3$, and $Fe_{65}Ni_{35}$ at room temperature are compared with those of the component elements Fe and Ni in Table I. Clearly the elastic behavior under pressure of the Invar alloys is completely different from those of the metals of the ferromagnetic elements. $(\partial C_{11}/\partial P)_{P=0}$ is a large negative quantity for the $Fe_{72}Pt_{28}$ and $Fe_{72}Pt_{25}Ni_3$ alloys, although for bcc Fe and fcc Ni it has the usual positive sign and has a magnitude in the range normally found for cubic metals. In the ferromagnetic phase pressure has the extremely unusual effect of reducing the longitudinal mode velocities and hence C_{11} and C_L. As a result the pressure derivative $(\partial B^S/\partial P)_{P=0}$ of the adiabatic bulk modulus B^S $(=(C_{11}+2C_{12})/3)$ is a large negative quantity [Fig. 1(a)]: this alloy becomes easier to compress as pressure is applied. In the case of $Fe_{65}Ni_{35}$ $(\partial B^S/\partial P)_{P=0}$ is slightly positive; however inspection of Renaud's[15] data shows that both the Invar alloys $Fe_{64}Ni_{36}$ and $Fe_{58}Ni_{42}$ in the ferromagnetic state have small negative values for $(\partial B^S/\partial P)_{P=0}$. The large negative $(\partial B^S/\partial P)_{P=0}$ (a newly recognized invar property in the Fe-Pt alloys)[10] relates directly to the negative thermal expansion: both properties involve the cubic term in the strain energy of the identical irreducible representation η_0^0, the volume strain $(\eta_{11}+\eta_{22}+\eta_{33})$ [Eq. (4)]. The negative thermal expansions of the $Fe_{72}Pt_{28}$ and $Fe_{72}Pt_{25}Ni_3$ alloys are consistent with the large negative values (-12.0 and -14.3, respectively) of the Slater gamma,[37] which is given in an isotropic Debye model by

$$\gamma_s = \left[\frac{1}{2}\right]\left[\frac{dB}{dP}\right] - \left[\frac{1}{6}\right] . \quad (8)$$

The overriding importance of volume strain in Invar behavior in the ferromagnetic state is emphasized by the finding that while $(\partial C_{11}/\partial P)_{P=0}$, $(\partial C_L/\partial P)_{P=0}$, and $(\partial B^S/\partial P)_{P=0}$ are all large negative quantities for $Fe_{72}Pt_{28}$ and $Fe_{72}Pt_{25}Ni_3$ alloys, the volume-conserving shear moduli C_{44} usually and C' always increase with pressure in the normal way (Tables II and III). In the paramagnetic phase all the elastic stiffnesses, and hence the mode frequencies and energies, increase with pressure. Thus the negative values of $(\partial C_{11}/\partial P)_{P=0}$ and $(\partial B^S/\partial P)_{P=0}$ found only in the ferromagnetic phase are a consequence of a magnetovolume interaction.

The pressure derivatives of the SOEC have been measured for $Fe_{72}Pt_{28}$ from 230 to 360 K, for $Fe_{72}Pt_{25}Ni_3$ from 250 to 340 K and for $Fe_{65}Ni_{35}$ at room temperature (Fig. 8). The pressure derivative $(\partial C'/\partial P)_{P=0}$ of the shear stiffness C' is almost independent of temperature.

However for $Fe_{72}Pt_{28}$ both $(\partial C_{11}/\partial P)_{P=0}$ and $(\partial C_L/\partial P)_{P=0}$ pass through a pronounced minimum at a temperature substantially below T_c, a feature which parallels the behavior of the thermal expansion.[16] The nonlinear acoustic properties can be correlated with the thermal expansion by recourse to the Grüneisen parameter approach and we now turn to that.

V. LONGITUDINAL ACOUSTIC MODE SOFTENING, GRÜNEISEN PARAMETERS, AND NEGATIVE THERMAL EXPANSION

A negative hydrostatic pressure derivative of an ultrasonic mode velocity and the associated elastic stiffness implies the unusual attribute that under induced stress the long wavelength acoustic mode frequencies $\omega_p(q)$ and energies decrease. The dependence of the acoustic mode frequency ω_i on volume can be expressed as a mode Grüneisen γ

$$\gamma_i = -\left[\frac{\partial \ln \omega_i}{\partial \ln V}\right]_T \tag{9}$$

which can be obtained from the measurements of the elastic stiffness tensor components and their dependences on pressure. In the anisotropic continuum model the mode γ_i for a cubic crystal are given by[38]

$$\gamma_i = (1/6w)(3B + 2w + k) , \tag{10}$$

where

$$w = C_{11}K_1 + C_{44}K_2 + C_{12}K_3 , \tag{11}$$

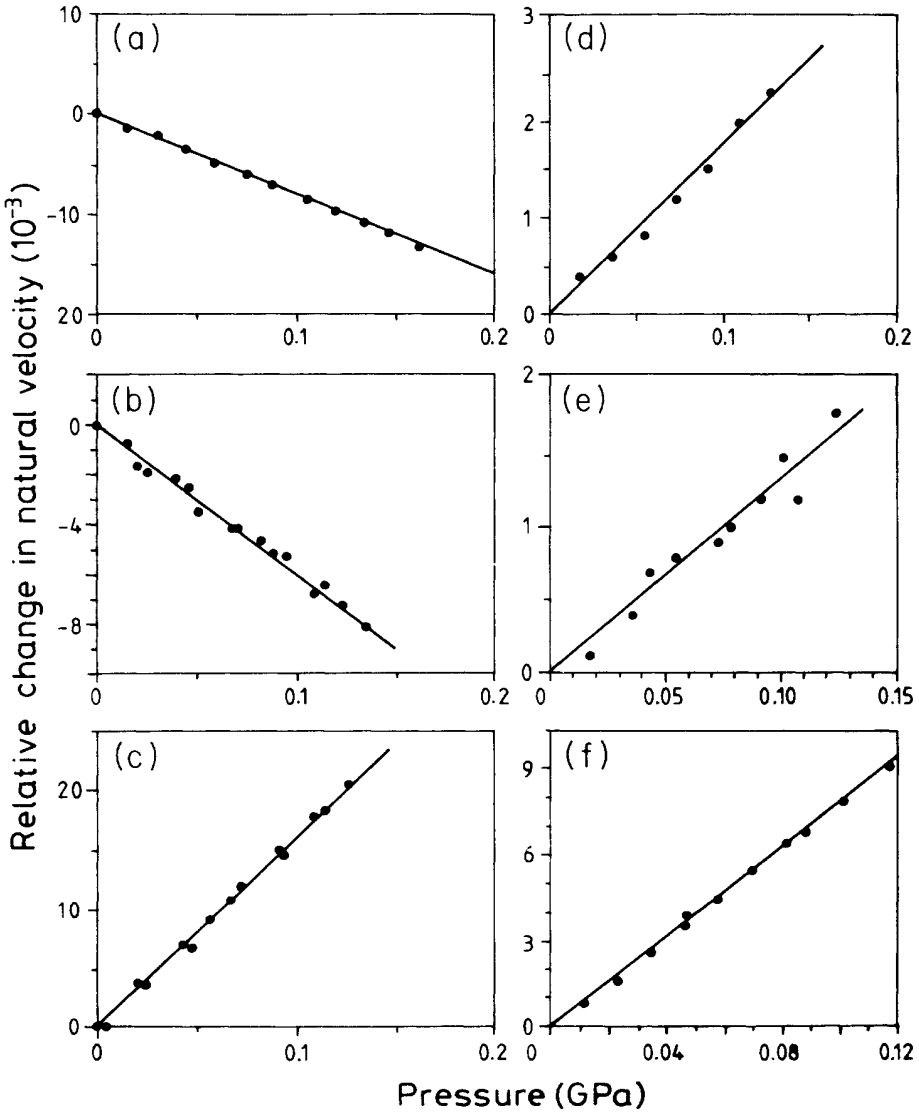

FIG. 7. The relative change with hydrostatic pressure in natural velocity of ultrasonic waves propagated in the ferromagnetic states at 293 K in monocrystalline $Fe_{72}Pt_{25}Ni_3$ (a) **N**[001], **U**[001], (b) **N**[110], **U**[110], (c) **N**[110], **U**[1$\bar{1}$0], and in monocrystalline $Fe_{65}Ni_{35}$ (d) **N**[001], **U**[001], (e) **N**[110], **U**[110], (f) **N**[110], **U**[1$\bar{1}$0].

$$k = C_1 K_1 + C_2 K_2 + C_3 K_3 \ , \tag{12}$$

with

$$K_1 = N_1^2 U_1^2 + N_2^2 U_2^2 + N_3^2 U_3^2 \ , \tag{13}$$

$$K_2 = (N_2 U_3 + N_3 U_2)^2 + (N_3 U_1 + N_1 U_3)^3 + (N_1 U_1 + N_2 U_1)^2 \ , \tag{14}$$

$$K_3 = 2(N_2 N_3 U_2 U_3 + N_3 N_1 U_3 U_1 + N_1 N_2 U_1 U_2) \ , \tag{15}$$

$$C_1 = C_{111} + 2C_{112} \ , \tag{16}$$

$$C_2 = C_{144} + 2C_{166} \ , \tag{17}$$

$$C_3 = C_{123} + 2C_{112} \ . \tag{18}$$

Here N_i and U_i are direction cosines for wave propagation and polarization directions, respectively. The third-order elastic constant combinations C_1, C_2, and C_3 [Eqs. (16), (17), and (18)] have been obtained using

$$(C_{111} + 2C_{112}) = -\left[2C_{11} + 2C_{12} + (C_{11} + 2C_{12}) \left[\frac{\partial C_{11}}{\partial P} \right]_{P=0} \right] , \tag{19}$$

$$(C_{144} + 2C_{166}) = -\left[C_{11} + 2C_{12} + C_{44} + (C_{11} + 2C_{12}) \left[\frac{\partial C_{44}}{\partial P} \right]_{P=0} \right] , \tag{20}$$

$$(C_{123} + 2C_{112}) = -\left[-C_{11} - C_{12} + (C_{11} + 2C_{12}) \left[\frac{\partial C_{12}}{\partial P} \right]_{P=0} \right] . \tag{21}$$

From the data obtained for the adiabatic SOEC elastic stiffnesses and their hydrostatic pressure derivatives the γ_i have been computed for $Fe_{72}Pt_{28}$ and $Fe_{72}Pt_{25}Ni_3$ as a function of mode propagation direction. The dependences upon the propagation vector $\mathbf{N}$ of the $\gamma(p,\mathbf{N})$ for each acoustic branch p near $\mathbf{k}=0$ in directions in the symmetry planes normal to the twofold and fourfold directions are plotted in Fig. 9 for $Fe_{72}Pt_{28}$ and for $Fe_{72}Pt_{25}Ni_3$ in Fig. 10. These Grüneisen parameters

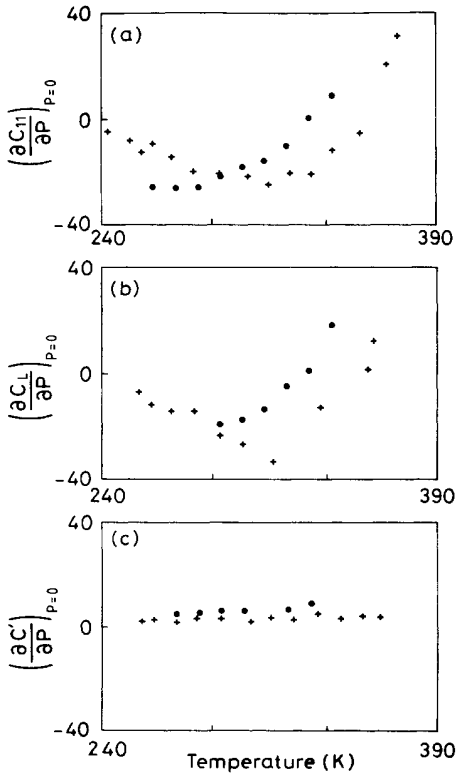

FIG. 8. Hydrostatic pressure derivatives of elastic stiffness tensor components of $Fe_{72}Pt_{28}$ (crosses) and $Fe_{72}Pt_{25}Ni_3$ (solid circles) as a function of temperature: (a) $(\partial C_{11}/\partial P)_{P=0}$, (b) $(\partial C_L/\partial P)_{P=0}$, (c) $(\partial C'/\partial P)_{P=0}$.

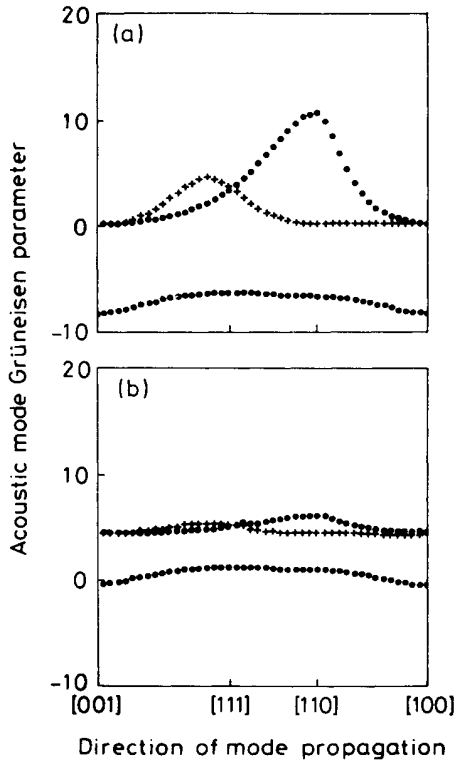

FIG. 9. Long-wavelength acoustic-mode Grüneisen parameters of $Fe_{72}Pt_{28}$ as a function of mode propagation direction (a) in the ferromagnetic state at 293 K: longitudinal (open circles) and shear (solid circles and crosses) modes and (b) in the vicinity of T_c at 360 K: longitudinal (open circles) and shear (solid circles and crosses) modes.

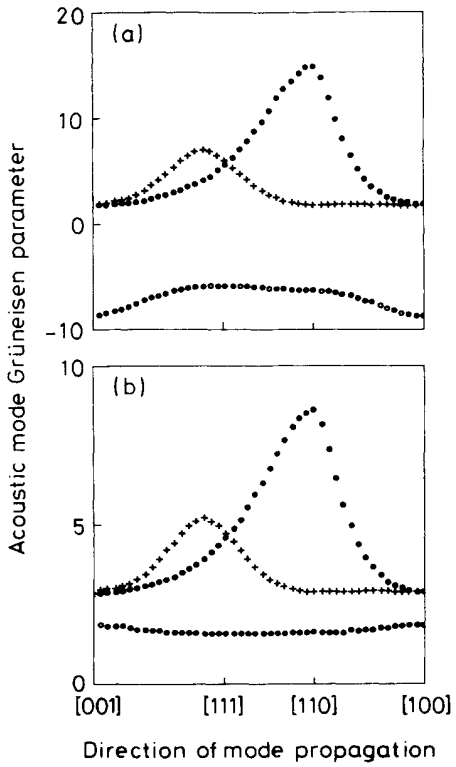

FIG. 10. Long-wavelength acoustic-mode Grüneisen parameters as a function of mode propagation direction in the ferromagnetic states at 293 K of (a) $Fe_{72}Pt_{25}Ni_3$ and (b) $Fe_{65}Ni_{35}$: longitudinal (open circles) and shear (solid circles and crosses) modes.

quantify the vibrational anharmonicity to first order (that is, for the cubic term in the strain Hamiltonian) of the acoustic modes at the Brillouin zone center. In the paramagnetic state the $\gamma(p,\mathbf{N})$ show normal behavior in all being positive: the mode frequencies and energies increase under pressure. However in the ferromagnetic state $Fe_{72}Pt_{28}$ (Fig. 9) and $Fe_{72}Pt_{25}Ni_3$ (Fig. 10) show the striking feature that all the longitudinal and quasilongitudinal long-wavelength modes have negative γ's. In this respect $Fe_{72}Pt_{28}$ and $Fe_{72}Pt_{25}Ni_3$ contrast markedly with the $Fe_{65}Ni_{35}$ alloy for which the pressure derivatives of the elastic constants (Table I), the mode Grüneisen parameters (Fig. 10), and the thermal expansion[1] are all positive.

The measurements of the hydrostatic pressure derivatives of the SOEC made for $Fe_{72}Pt_{28}$ from 230 to 360 K and for $Fe_{72}Pt_{25}Ni_3$ from 250 to 340 K, shown in Fig. 8, enable determination of the acoustic mode Grüneisen parameters over these temperature ranges. For both $Fe_{72}Pt_{28}$ and $Fe_{72}Pt_{25}Ni_3$ the temperature dependence of the Grüneisen gamma $\gamma_L[100]$ of the longitudinal mode propagated in a $\langle 100 \rangle$ direction remains negative from 220 K up to T_c passing through a minimum at about 315 K (Fig. 11). As the temperature is raised, the hydrostatic pressure derivatives of the longitudinal mode velocities and hence their Grüneisen γ's decrease and eventually just below T_C the diminishing magnetoelastic interaction which leads to the longitudinal mode softening is counterbalanced by the more usual positive contribution from vibrational anharmonicity; therefore the longitudinal mode γ's become positive close to the transition to the paramagnetic state. The pressure derivative also shows a broad minimum in this temperature range [Fig. 11(c)].

There is a direct link between the longitudinal mode softening and the negative thermal expansion which also is due to the anharmonicity of lattice vibrations but includes contributions from phonons of wave vectors spanning the entire Brillouin zone in all branches. In the quasiharmonic approximation the corresponding thermal

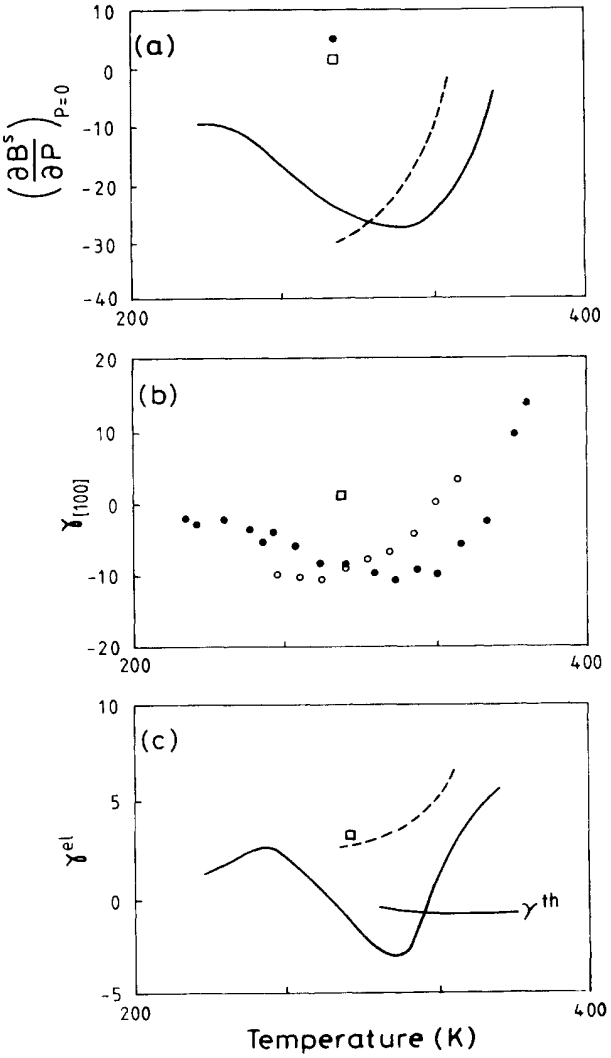

FIG. 11. The temperature dependences of (a) the hydrostatic pressure derivative $(\partial B^S/\partial P)_{P=0}$ of the adiabatic bulk modulus (solid line: $Fe_{72}Pt_{28}$; dotted line: $Fe_{72}Pt_{25}Ni_3$; square: Fe; solid circle: $Fe_{65}Ni_{35}$), (b) the long-wavelength longitudinal acoustic-mode Grüneisen gamma $\gamma_L[100]$ (solid circles: $Fe_{72}Pt_{28}$; open circles: $Fe_{72}Pt_{25}Ni_3$; square: $Fe_{65}Ni_{35}$), and (c) the mean elastic Grüneisen parameter γ^{el} (solid line: $Fe_{72}Pt_{28}$; dotted line: $Fe_{72}Pt_{25}Ni_3$; square: $Fe_{65}Ni_{35}$) and the thermal Grüneisen parameter γ^{th}.

Grüneisen parameter γ^{th} is the weighted average, given by Eq. (2), of all the individual excited mode (i) Grüneisen parameters γ_i [Eq. (9)]. At high temperatures ($T \gg \Theta_D; \Theta_D^{el}$ about 320 K) the heat capacity C_i per mode becomes equal to the Boltzmann constant. The thermal Grüneisen parameter γ^{th} has been determined using thermal expansion, specific heat (W. Pepperhoff, private communication) and bulk modulus data in Eq. (1) and is compared with γ^{el} in Fig. 11(c). The temperature dependence of the thermal expansion can be understood in the following way. As temperature is reduced, optical phonons freeze out first and their contributions, and those of the population of the large wave vector **k** acoustic mode phonons of higher energy, to γ^{th} and β decrease, so that the long-wavelength acoustic phonons, whose Grüneisen γ's are shown in Figs. 9 and 10 for $Fe_{72}Pt_{28}$ and $Fe_{72}Pt_{25}Ni_3$, respectively, play an increasingly important role. The temperature dependence of the mean long-wavelength acoustic-mode Grüneisen parameter γ^{el}, given by the sum $(1/12\pi)\sum_{ZCM}\int\gamma(p,\mathbf{N})d\Omega$ over all zone-center modes (ZCM), is shown in Fig. 11(c). The thermal expansion results from the mutual cancellation of effects from modes having Grüneisen parameters some of negative and others of positive sign. In the summation [Eq. (2)] yielding γ^{th}, the influence of the longitudinal modes, which have negative Grüneisen γ's in the ferromagnetic state, overrides that from the transverse modes which have positive but numerically smaller $\gamma(p,\mathbf{N})$ (Figs. 9 and 10). Further confirmation that the negative thermal expansion does indeed result from the soft longitudinal mode contributions comes from consideration of the temperature range over which the effect occurs. The markedly sample-dependent thermal expansion in a $Fe_{72}Pt_{28}$ specimen was found to be negative between about 260 and 376 K with a minimum at about 350 K.[14] $Fe_{72}Pt_{25}Ni_3$ shows similar behavior.[16] Inspection of the temperature dependences of γ_L [100] and γ^{el} (Fig. 11) shows why negative thermal expansion occurs only in this restricted range. While γ_L [100] remains negative down to 220 K it has a comparatively small value at the lower temperatures so that γ^{el}, which sums over both longitudinal and shear modes, becomes positive again. There is a range of temperature in which the contribution of the longitudinal acoustic modes causes the thermal expansion to be negative. The combination of reduction of the longitudinal Grüneisen parameters and freeze out of these modes at low temperature leads to domination by the lower energy transverse acoustic modes with positive Grüneisen parameters, so that the thermal expansion resumes the normal positive sign.

While this experimental work has been in progress there has been a relevant development in theoretical understanding of the anomalous volume behavior of Invars in terms of itinerant electron magnetism.[6] In general the volume thermal expansion coefficient β is given by

$$\beta=\frac{1}{B}\left[\frac{\partial P_{el}}{\partial T}+\frac{\partial P_{ph}}{\partial T}\right]=\beta_{el}+\beta_{ph}\ , \tag{22}$$

where $P_{el}(=-\partial F_{el}/\partial V)$ and $P_{ph}(=-\partial F_{ph}/\partial V)$ are the pressures due to the electrons and phonons, respectively, F being the free energy. Throughout the long list of theoretical models trying to solve the Invar problem it has been customary to attribute the origin of the anomalous volume behavior solely to the electron contribution, while assuming that β_{ph} behaves normally even in the ferromagnetic state. Kim[6] has proposed that the phonon contribution to the free energy of a ferromagnetic metal, as well as that from electrons, must also depend on magnetization. He finds that the theory of itinerant electron ferromagnetism in circumstances that apply to Fe_3Pt predicts negative longitudinal mode Grüneisen parameters due to the magnetoelastic interaction, as observed experimentally,[9,10] and hence to a negative thermal expansion. For Fe_3Pt in particular a numerical but qualitative calculation based on a model density of states function with two maxima in the band does predict a negative phonon Grüneisen parameter, its actual value and hence that of β_{ph} being very sensitive on the location of the Fermi energy. Although Kim has directed his attention to understanding bulk effects, in particular volume expansion and bulk modulus, in fact his approach using the jellium model restricts his argument to longitudinal acoustic phonons because these are the only modes which can propagate. Hence his prediction actually refers to a negative Grüneisen parameter for these particular phonons in the ferromagnetic state—the pressure dependences of longitudinal wave velocities found here not only establish that this is true but also measure quantitatively the mode parameters themselves. This accord between experiment and theory indicates strongly that the Invar effects in Fe-Pt alloys result directly and naturally from contributions from the soft longitudinal acoustic phonons outwaying those from other modes which may show the more usual positive dependence of frequency upon volume or pressure.

To conclude, acoustic mode softening plays a dominant role in the elastic behavior and phase stability of Fe-Pt and Fe-Ni alloys. Longitudinal mode softening is intimately bound up with the Invar properties in the ferromagnetic state. Shear mode softening drives the martensitic fcc-bct structural transition.

ACKNOWLEDGMENTS

We are grateful to the British Council, MEC (Spain) and the Deutsche Forschungsgemeinschaft (SFB166) for financial support. We would also like to thank E. F. Lambson and R. C. J. Draper for technical assistance.

*On leave from the Department d'Estructura i Constituents de la Matèria, Facultat de Física, Universitat de Barcelona, Catalonia, Spain.

[1]C. E. Guillaume, C. R. Acad. Sci. Paris **125**, 235 (1897).
[2]C. E. Guillaume, C. R. Acad. Sci. Paris **170**, 1554 (1920).
[3]E. F. Wasserman, Phys. Scr. T **25**, 209 (1988).
[4]G. Hausch, J. Phys. Soc. Jpn. **37**, 819 (1974).
[5]E. P. Wohlfarth, Physica **119B**, 203 (1983).

[6]D. J. Kim, Phys. Rev. B **39**, 6844 (1989).
[7]M. Shiga, K. Makita, K. Uematsu, Y. Muraoka, and Y. Nakamura, J. Phys: Condens. Matter **2**, 1239 (1990).
[8]A. Z. Menshikov, Physica B **161**, 1 (1989).
[9]U. Kawald, J. Pelzl, G. A. Saunders, P. Ngoepe, and H. Rahdi, in *Phonons 89*, Proceedings of the 3rd International Conference on Phonon Physics and the 6th International Conference on Phonon Scattering in Condensed Matter, edited by S. Hunklinger, W. Ludwig, and G. Weiss (World Scientific, Singapore, 1989), Vol. 2, p. 1111.
[10]Ll. Mañosa, G. A. Saunders, H. Radhi, U. Kawald, J. Pelzl, and H. Bach, J. Phys.: Condensed Matter **3**, 2273 (1991).
[11]S. Chikazumi, T. Mizoguchi, N. Yamaguchi, and P. Beckwith, J. Appl. Phys. **39**, 939 (1968).
[12]Y. Nakamura, IEEE Trans. Magn. **MAG-12**, 278 (1976).
[13]E. F. Wasserman, Festkörperprobleme **27**, 85 (1987).
[14]K. Sumiyama, M. Shiga, M. Morioka, and Y. Nakamura, J. Phys. F **9**, 1665 (1979).
[15]P. Renaud, Ph.D. thesis, Universite de Lausanne, Switzerland (1988).
[16]A. P. Miodownik, J. Magn. Magn. Mater **10**, 126 (1979).
[17]M. Hansen, *Constitution of Binary Alloys* (McGraw-Hill, New York, 1958).
[18]G. Hausch and H. Warlimont, Acta Metall. **21**, 401 (1973).
[19]U. Kawald, W. Zemke, H. Bach, J. Pelzl, and G. A. Saunders, Physica B **161**, 72 (1989).
[20]S. Muto, R. Oshima, and F. E. Fujita, Metall. Trans. **19A**, 2723 (1988).
[21]E. P. Papadakis, J. Acoust. Soc. Am. **42**, 1045 (1967).
[22]E. Kittinger, Ultrasonics **15**, 30 (1977).
[23]S. C. Flower and G. A. Saunders, Philos. Mag. B **62**, 311 (1990).
[24]G. A. Alers and J. R. Neighbours, J. Phys. Chem. Solids **13**, 40 (1960).
[25]G. Hausch and H. Warlimont, Phys. Lett. **41A**, 437 (1972).
[26]R. F. S. Hearmon, *Elastic, Piezoelectric, Pyroelectric, Piezooptic, Electrooptic Constants and Nonlinear Dielectric Susceptibilities of Crystals*, Springer-Verlag, Berlin, Vol. 11 of Londolt-Börnstein New Series, edited by K.-H. Hellwege (Springer-Verlag, Berlin, 1979), p. 11.
[27]R. A. Macfarlane, J. A. Rayne, and C. K. Jones, Phys. Lett. **18**, 91 (1965).
[28]R. D. Lowde, R. T. Harley, G. A. Saunders, M. Sato, R. Scherm, and C. Underhill, Proc. R. Soc. London, Ser. A **374**, 87 (1981).
[29]M. Sato, R. D. Lowde, G. A. Saunders, and M. M. Hargreave, Proc. R. Soc. London, Ser. A **374**, 115 (1981).
[30]N. Boccara, Ann. Phys. (N.Y.) **47**, 40 (1968).
[31]J. Liakos and G. A. Saunders, Philos. Mag. A **46**, 217 (1982).
[32]M. P. Brassington and G. A. Saunders, Phys. Rev. Lett. **48**, 159 (1982).
[33]M. P. Brassington and G. A. Saunders, Proc. R. Soc. London, Ser. A **387**, 289 (1983).
[34]R. A. Cowley, Phys. Rev. B **13**, 4877 (1976).
[35]G. Oomi and N. Mori, J. Phys. Soc. Jpn. **50**, 2917 (1981).
[36]R. N. Thurston, Proc. IEEE **53**, 1320 (1965).
[37]J. C. Slater, *Introduction to Chemical Physics* (McGraw-Hill, New York, 1939).
[38]K. Brugger and T. C. Fritz, Phys. Rev. **157**, 524 (1967).